JEFFREY L. HANSON

WINDS, WAVES, AND BUBBLES AT THE AIR-SEA BOUNDARY

Subsurface bubbles are now recognized as a dominant acoustic scattering and reverberation mechanism in the upper ocean. A better understanding of the complex mechanisms responsible for subsurface bubbles should lead to an improved prediction capability for underwater sonar. The Applied Physics Laboratory recently conducted a unique experiment to investigate which air-sea descriptors are most important for subsurface bubbles and acoustic scatter. Initial analyses indicate that wind-history variables provide better predictors of subsurface bubble-cloud development than do wave-breaking estimates. The results suggest that a close coupling exists between the wind field and the upper-ocean mixing processes, such as Langmuir circulation, that distribute and organize the bubble populations.

INTRODUCTION

A multiyear series of experiments, conducted under the auspices of the Navy-sponsored acoustic program, Critical Sea Test (CST),[1] has been under way since 1986 with the charter to investigate environmental, scientific, and technical issues related to the performance of low-frequency (100–1000 Hz) active acoustics. One key aspect of CST is the investigation of acoustic backscatter and reverberation from upper-ocean features such as surface waves and bubble clouds. It is assumed that a better understanding of the complex mechanisms of the upper ocean will lead to an improved ability to predict surface backscatter.

The Applied Physics Laboratory has played a lead role in the design, conduct, and ongoing analysis of the air-sea environmental measurements in support of the CST acoustic scatter and reverberation research. The Critical Sea Test 7 (CST-7) Phase 2 experiment, conducted by APL from 24 February through 1 March 1992 in the Gulf of Alaska, was designed specifically to investigate the mechanisms of surface acoustic scatter and reverberation at frequencies below 1000 Hz.[2,3] In particular, the development and evolution of subsurface bubble clouds, known to be a dominant scatter mechanism,[4,5] were observed in conjunction with low-frequency acoustic backscatter measurements. The experiment provided a first-time opportunity to combine the open-ocean acoustic measurement capabilities of the CST program with state-of-the-art air-sea boundary instrumentation and the theoretical developments of scientists conducting basic research.

As a first step in analyzing the results from CST-7, an empirical evaluation was performed on the relationships between atmospheric forcing and the resulting sea-surface response in terms of wave growth, wave breaking, and the development of subsurface bubble features. The results provide interesting clues to the nature of the coupling between the atmosphere and the ocean. It is found that, in the Gulf of Alaska wintertime environment, the amount of wave-breaking activity may not be an ideal indicator of deep bubble-cloud formation. Instead, the penetration of bubbles is more closely tied to short-term wind fluctuations, suggesting a close coupling between the wind field and upper-ocean mixing processes that distribute and organize the bubble populations within the mixed layer.

BACKGROUND

Sea-surface scattering results from the interaction of acoustic energy with features at or near the ocean surface. In particular, subsurface bubbles have been shown to cause elevated levels of low-frequency acoustic scatter in theory,[4] in carefully controlled lake experiments,[5] and in the open ocean at high wind speeds.[6] Clearly, the process is complex because of the dynamic nature of the air-sea boundary zone. This section is a synopsis of the mechanisms thought to be important for the development of subsurface bubble structures and hence increased levels of acoustic scatter.

Within the air-sea boundary zone, several complex physical, chemical, and biological processes interact to form a given set of environmental conditions. Of key importance to understanding the mechanisms related to subsurface bubbles is the original input of energy to the system. Two dominant mechanisms are involved: the transfer of mechanical energy by the wind, and the radiation of heat energy from the Sun.

As Figure 1 indicates, the stress applied on the ocean surface by a given wind is influenced by the stability of the atmosphere above the ocean surface. A good review of atmospheric boundary-layer theory is given by Stull.[7] The atmosphere-ocean coupling induced by the wind results in the growth of wind waves[8] and in the development of a surface drift current.[9]

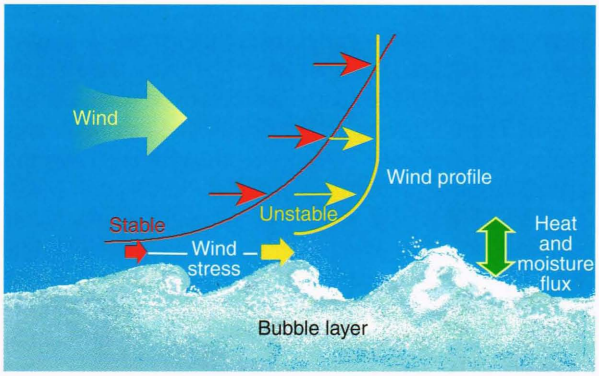

Figure 1. Atmospheric forcing and the development of a subsurface bubble layer by breaking waves. Shipboard measurement elevation = 19.5 m.

The wind energy delivered to the surface wave field is dissipated through wave breaking.[10] Significant quantities of air can be entrained by a breaking wave, resulting in the injection of dense bubble plumes into the upper water column. Laboratory experiments suggest that interaction with ocean swell may substantially alter the breaking characteristics of wind waves, although the exact mechanisms are not yet known.[11]

Several processes occur once air is introduced into the mixed layer by breaking waves. Buoyancy drives the larger bubble assemblages immediately back to the sea surface. The remaining bubbles either go into solution at a rate governed by the gas solubility properties of the surrounding water or become stabilized by surfactants.[12] The bubbles that persist become entrained in the local turbulent field. Langmuir circulation cells have been observed to organize microbubble assemblages into semicoherent structures extending several meters below the surface.[12–14] As Figure 2 shows, the downwelling regions are marked by sea-surface streaks, or "wind rows," that form along Langmuir cell convergence zones nearly parallel to the wind direction. Langmuir cells are thought to be formed and maintained through a nonlinear interaction between the wind-induced surface drift and the surface-wave Stokes drift,[15] thus linking subsurface bubble structures with the surface wind and wave fields.

This intricate atmosphere–mixed layer coupling has been highly oversimplified in the field of acoustic propagation modeling. As Figure 2 indicates, the air-water interface, dense bubble plumes beneath breaking waves, tenuous microbubble clouds extending into the mixed layer, and upper-ocean fish populations are all features that may cause elevated scatter and reverberation. Presently, short-term average wind speed measured at a standard reference height above the ocean surface (19.5 m) is the sole environmental variable used in the prediction of acoustic scatter in most operational models.[6] The effects of wind history, surface-wave interactions, and mixed-layer heating and cooling that alter the intensity and structure of subsurface bubble features are completely ignored. It is not surprising that model predictions of surface backscatter at a particular site can be 10 to 15 dB off from measured values (P. Ogden, pers. comm., 1993).

HYPOTHESIS AND RESEARCH OBJECTIVE

The hypothesis under investigation is that predictions of low-frequency acoustic surface scatter can be improved by replacing the single environmental parameter, instantaneous wind speed, with an improved sea-state descriptor that includes the effects of wind history, wave-field development and directionality, and mixed-layer properties (depth, temperature, and stability). A primary objective of CST-7, therefore, was to observe and describe carefully the state and evolution of the air–sea boundary zone over the experimental duration. The observations involved an intensive suite of air–sea measurements made from ships, aircraft, and drifting instruments.

The physical relationship of specific features to the complex interactions of the air–sea boundary zone, and in particular the existence of subsurface bubble features and their significance for acoustic surface scatter, is the subject of ongoing analyses and will be addressed more fully in future publications. The objective of the work reported here is to investigate empirically the coupling between the observed wind field and the development of

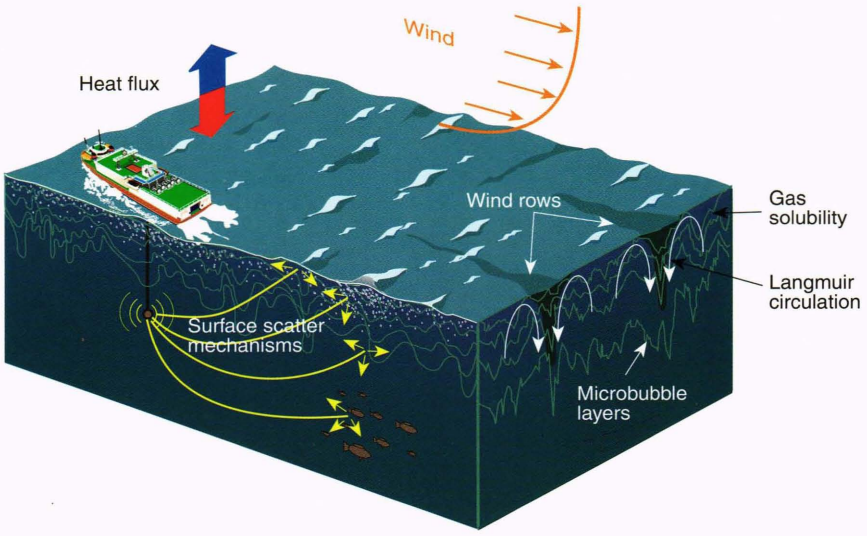

Figure 2. Acoustic scatter in the upper ocean is thought to be influenced by surface waves, dense bubble plumes beneath breaking waves, subsurface microbubble clouds organized by Langmuir circulation, and fish populations.

surface waves, the degree of wave breaking, and the development of subsurface bubble clouds. The findings from this study should provide useful guidance for conducting a more intensive physics-based analysis now planned for the CST-7 results.

EXPERIMENTAL OVERVIEW

The CST-7 test site in the dynamic environment of the central Gulf of Alaska was chosen in hopes of experiencing a wide variety of air-sea conditions (Fig. 3). Site selection was influenced by historical weather information (we were looking for adverse weather!) and the need for deep water with an Arctic half-channel-like sound-speed profile to limit bottom reverberation and maximize acoustic interaction with the surface.

The experimental scenario is depicted in Figure 4. Participating in the test were U.S. and Canadian research vessels as well as ships and aircraft of the U.S. Navy.

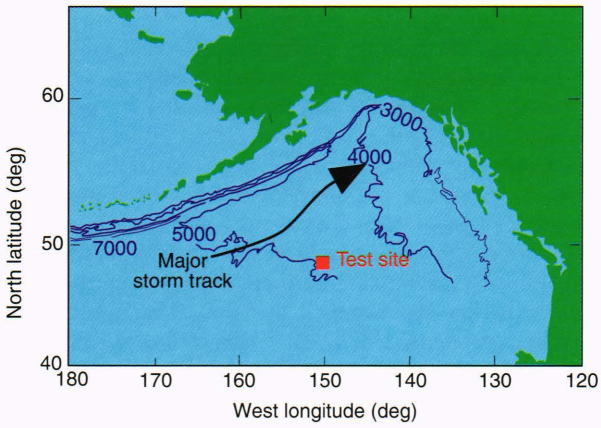

Figure 3. The Gulf of Alaska surface scatter and air-sea interaction experiment (Critical Sea Test 7, Phase 2) was conducted by APL from 24 February through 1 March 1992 in the Gulf of Alaska. The numbers on the map are bathymetric contours in meters.

A series of carefully planned environmental measurements and acoustic scatter experiments were simultaneously conducted to allow investigation of the effects of particular air-sea boundary features on surface acoustic scatter. The CSS *John P. Tully* deployed and maintained a suite of sophisticated air-sea boundary zone instrumentation within 20 km of the designated center point (48°45' N, 150°00' W). The R/V *Cory Chouest* conducted the principal acoustic experiments in a manner that often placed the surface-scatter patch in the region of the air-sea boundary instruments. The P-3 aircraft conducted valuable wide-area oceanographic and environmental-acoustic surveys of the experimental site. The remaining platforms, although dedicated to the acoustic experiments, also made standard shipboard environmental measurements.

The key environmental measurements and the principal investigators are listed in Table 1. Of particular importance was the characterization of the subsurface bubble layers at a time and location nominally coincident with the acoustic scatter experiments. In turn, the dominant forcing processes thought to precipitate and modify the subsurface bubble layers (e.g., winds, waves, and stability) were also observed. The specific instruments that gathered data to produce the initial results presented here are described in the following paragraphs.

Shipboard air-sea boundary studies were conducted by using the personal-computer-based Air-Sea Dynamics System (ASDS)[16] developed at APL for the CST Program. The ASDS real-time processor accepts inputs from a wide variety of precision-calibrated, carefully placed air-sea sensors and incorporates a marine atmospheric boundary-layer model (bulk formulas) to generate profiles of surface-layer quantities (wind speed, temperature, and humidity), normalize meteorological measurements to common reference elevations, and compute various boundary-layer parameters such as atmospheric stability and wind stress. System validations are performed through

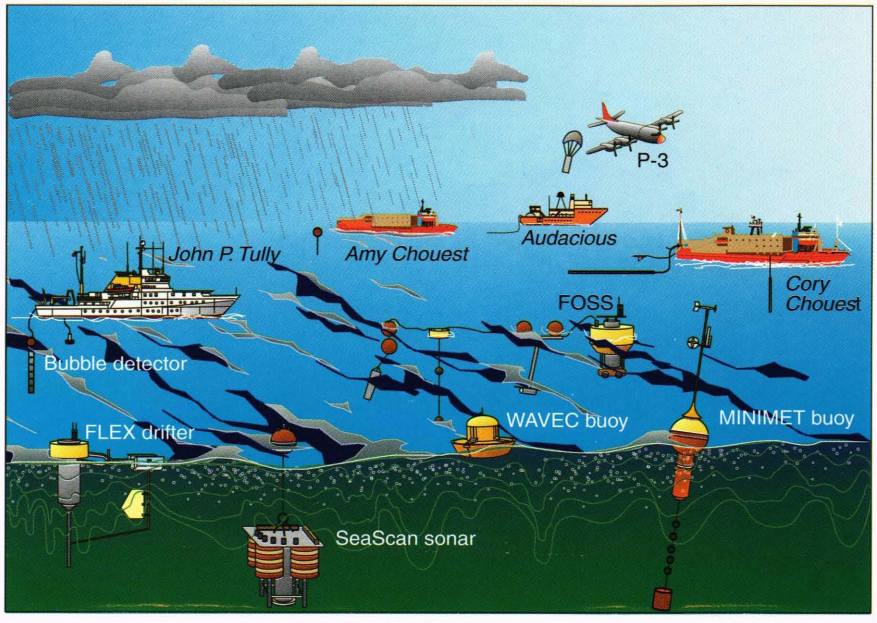

Figure 4. Test scenario for the Gulf of Alaska surface scatter and air-sea interaction experiment (Critical Sea Test 7, Phase 2). Open-ocean acoustic measurement capabilities of the Critical Sea Test Program were combined with state-of-the-art air-sea boundary measurements from scientists conducting basic research. FOSS = Forward Ocean Scatter System.

Table 1. CST-7 Phase 2 environmental measurement summary.

Technical issue	Approach	Principal investigator
Subsurface bubbles	SeaScan bubble sonar	D. Farmer,[a] S. Vagle (IOS)
	Bubble resonator array	M. Su (NRL-SSC)
Breaking waves	Whitecap video	E. Monahan (UCONN)
	FLEX void-fraction drifter	D. Farmer (IOS)
Surface wave field	Datawell WAVEC buoy	R. Marsden (RRMC)
	TSK shipboard wave radar	J. Hanson[b] (JHU/APL)
	Endeco 1156 wave buoy	
Wind speed/direction and meteorology	MINIMET buoy	D. Farmer (IOS)
	Shipboard air-sea dynamics systems	L. White (SAIC)
High-resolution wind stress	Fast-sample anemometer	R. Marsden (RRMC)
Water column structure and dissolved gas	System for At-Sea Environmental Analysis (SASEA)—XBT/XCTD/AXBT	M. Mandelberg (JHU/APL)
	CTD/dissolved oxygen	D. Farmer (IOS)
	POCO AMIGO Airborne System	N. Bedford (ARL/UT)

Note: TSK = TSKAmerica, XBT = expendable bathythermograph, CTD = conductivity-temperature-depth, XCTD = expendable CTD, AXBT = aircraft XBT, POCO AMIGO = portable, compact, acoustic measurement instrument for general operations, IOS = Institute of Ocean Sciences, NRL-SSC = Naval Research Laboratory-Stennis Space Center, UCONN = University of Connecticut, RRMC = Royal Roads Military College, SAIC = Science Applications International Corp., ARL/UT = Applied Research Laboratories/University of Texas at Austin.
[a]Chief Scientist on R/V *John P. Tully.*
[b]Environmental Measurement Coordinator.

comparison of ASDS measurements with NOAA data buoy and MINIMET weather buoy (Coastal Climate Co.) observations obtained in the vicinity of the *Cory Chouest,* as well as with direct wind stress measurements obtained with an onboard fast-sample anemometer. The results of these calibrations, presently in preparation for future publication, show that ASDS measurements are of higher quality than conventional shipboard observations.

For atmospheric and sea-surface measurements near the test center, a MINIMET meteorological buoy was deployed by the *John P. Tully*. The MINIMET is a free-drifting weather station complete with internal data processing and recording. Measured parameters included wind speed and direction, air temperature, sea-surface temperature, and barometric pressure. The MINIMET buoy was deeply drogued to minimize advection by near-surface currents and allowed to drift free near the test center. The MINIMET results were processed by using the ASDS boundary-layer model for wind-speed height normalization as well as by computation of wind stress and related parameters. The resulting wind speeds at the 19.5-m reference height, from MINIMET, appear in Figure 5 along with the deployment times for the instruments described in the following paragraphs.

A Datawell WAVEC heave, pitch, and roll buoy (2-m discus) deployed from the *John P. Tully* continuously measured wave height and direction over the experimental period. The WAVEC can measure 0.033- to 0.400-Hz ocean waves with a wave directional resolution of about 9°. Like MINIMET, the instrument was drogued at 165 m to minimize drift away from the test center. Wave statistics and directional spectra were computed by using a data-adaptive eigenvector technique.[17] The resulting series of 238 half-hourly directional spectra cover most of the experimental time period (Fig. 5). A spectral partitioning algorithm, based on that described by Gerling,[18] was applied to the WAVEC results so that separate statistics could be generated for the individual wind-sea and swell systems passing through the test site. The results provide a striking overview of the dynamic CST-7 wave field and aid in the interpretation of the present findings (see the next section).

To obtain information on the frequency of occurrence and the intensity of wave breaking, the experimental FLEX

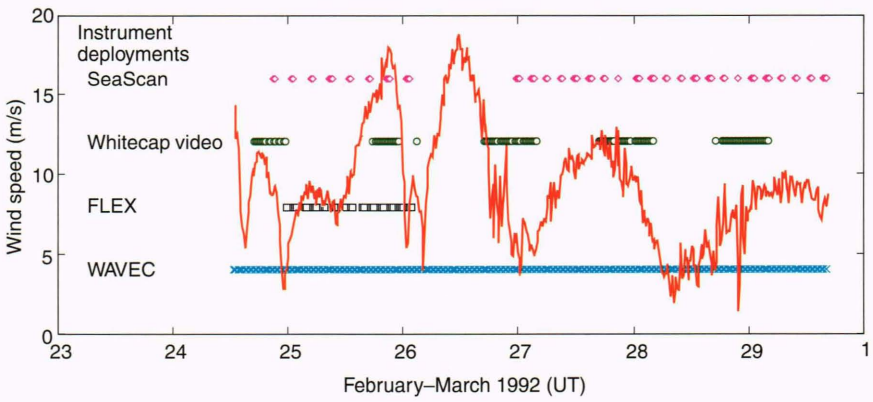

Figure 5. Air-sea instrument deployment times in relation to wind-speed history.

instrument was deployed from the *John P. Tully*. The FLEX has an array of four conductivity-thermistor cells mounted at depths from 0.15 to about 2 m on a freely floating frame. The instrument provides a Lagrangian measurement of the air void fraction injected by breaking waves into the upper 2 m of the water column and allows investigations into the frequency and duration of those wave-breaking events. Wave-breaking statistics, averaged over 15-min intervals, were computed for the deployment periods indicated in Figure 5.

To investigate further the mechanisms of bubble production through wave breaking, continuous video recordings of the sea surface were obtained during daylight hours by video camera systems mounted in heated instrument shelters on the sides of the *John P. Tully* and the *Cory Chouest*. The video images were analyzed by using an image-processing technique to evaluate the fraction of the sea surface covered by Stage A (active spilling crest) whitecaps[19] during the experiment. The observation times of the resulting data appear in Figure 5.

To map out the microbubble (8–150 μm radius) field from 1 to 2 m below the surface to a depth of about 30 m, the SeaScan subsurface microbubble sonar was deployed and allowed to drift free from the *John P. Tully*. SeaScan employs six upward-looking sonars operating at frequencies of 27.5, 52.4, 88.2, 132.0, 210.0, and 397.0 kHz to determine the bubble size distribution as a function of depth.[20] In addition, two orthogonal 100-kHz sidescan sonars look out horizontally to obtain the two-dimensional structure of near-surface features such as bubble rows organized by Langmuir circulation. Finally, an S4 current meter was mounted just below the sonar system to determine the velocity at which bubble features are advected past the instrument. For the present analysis, the 88.2-kHz sonar results were used with a low threshold to determine the average maximum depth of bubble penetration over 15-min intervals. Observation times for those results appear in Figure 5.

AIR-SEA CONDITIONS

The winter weather we experienced in the Gulf of Alaska was controlled by the passage of numerous atmospheric low-pressure systems, or "lows," moving through the region. The most severe influenced the experiment for a thirty-hour period from 25 to 26 February. The structure of that storm as it passed northward over the test site, at a speed of about 12 m/s, is depicted by the NOAA surface-pressure maps of Figure 6. A single low-pressure cell with associated atmospheric fronts dominated the weather in nearly the entire Gulf.

Selected meteorological and sea-surface records from the experiment appear in Figure 7. The test site was influenced by several lows during the six-day experiment. The first two, encountered on 24 and 26 February, passed almost directly over the test site and had the most significant effect on meteorological conditions. Note in particular the rapid air-temperature changes caused by the atmospheric fronts associated with the two lows. On average, air temperatures were 1.5°C cooler than sea-surface temperatures, resulting in slightly unstable atmospheric conditions and causing a small average heat loss from the ocean surface over the experimental period (L. White, pers. comm., 1993).

The passing lows produced a notable variability in wind speed and direction (Fig. 7), and elevated wind events were associated with each passing storm. The most significant of these were the two approximately twelve-hour high-wind episodes accompanying the 25 to 26 February winter storm. Winds were initially out of the north, and then temporarily plummeted as the eye of the storm passed over the site at about 0600 UT on 26 February. They then redeveloped from the west with peak speeds of 18 m/s (at 19.5-m height).

Of particular importance for this study is the effect of the meteorological events on the ocean surface. The significant wave-height record of Figure 7 indicates that surface waves peaked at 5.5 m as a result of the 25 to 26 February storm. Wave heights did not develop as dramatically during the other high-wind events, because the winds were either too low or unsteady, or varied in direction. Even during times of low winds, significant wave heights were at least 2 m because of ocean swells continually propagating through the Gulf.

To reveal the full dynamic nature of the sea surface during the experiment, the wave spectral partitioning results (see the "Experimental Overview" section) are

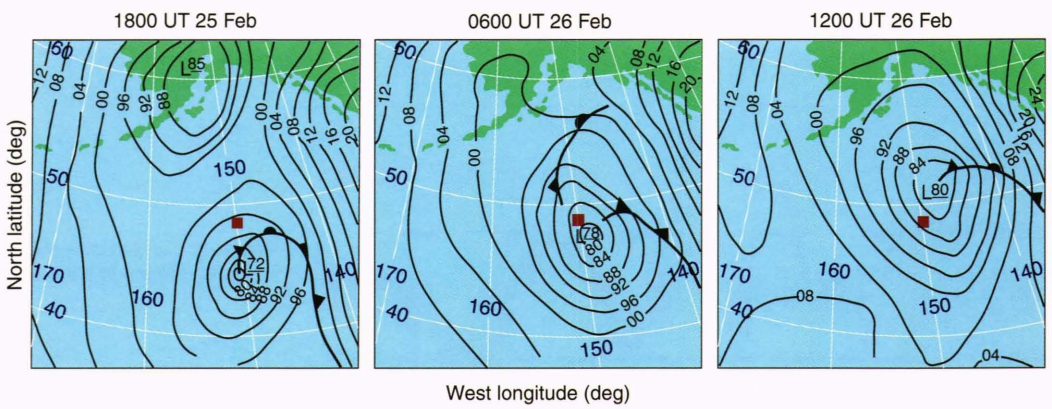

Figure 6. NOAA surface pressure maps showing the passage of the winter storm of 25 to 26 February 1992. This single storm covered nearly the entire Gulf of Alaska. The numbers on the isobars are the last two digits of the surface pressure in millibars.The test site is indicated by a red square.

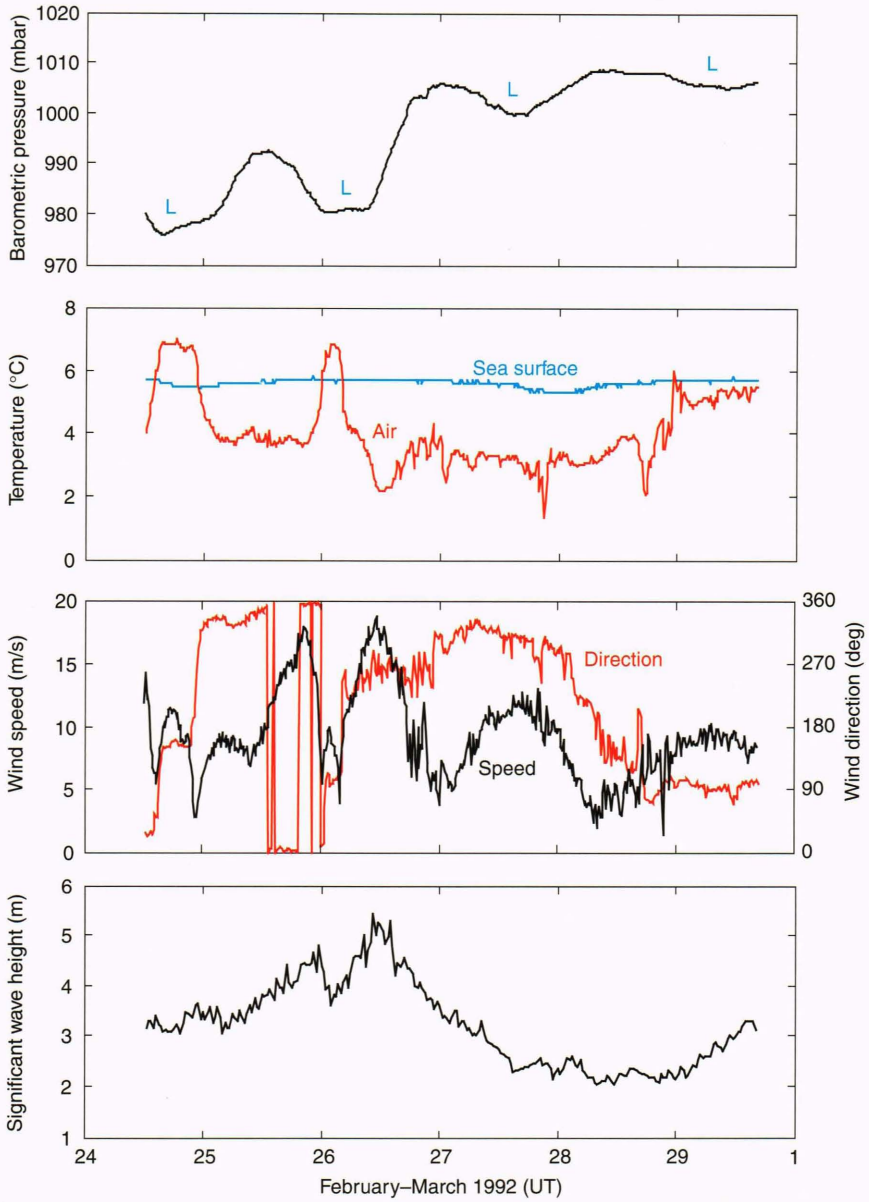

Figure 7. Selected meteorological and sea-surface records from Critical Sea Test 7, Phase 2.

presented in Figure 8. The wave-vector history reveals the evolution of various wave systems in terms of mean height (proportional to length of arrow), mean direction, and peak frequency. Note the general complexity of the wave field—up to four wave systems were moving through the test area at any given instant. Rapidly growing wind-wave systems result from elevated wind events (see Fig. 7). These wind seas often occurred in conjunction with multiple swells of similar height from local and distant storms. The slow shift to higher frequencies of swell systems from distant storm events is explained by the deep-water gravity wave relationship $C_p = g/2\pi f$, which states that wave phase speed (C_p) is inversely proportional to wave frequency (f), resulting in a progressive arrival of waves from low to high frequency.

The complex interactions between wind, wind waves, and swell result in wave-breaking and the injection of bubbles into the upper ocean. As previously noted, two separate indicators of wave-breaking activity were obtained during CST-7: wave-breaking frequency as measured *in situ* by the FLEX drifter, and surface whitecap fraction (active spilling crests) as remotely sensed by shipboard video. In addition, subsurface bubble-cloud depths have been estimated from the SeaScan sonar results. The variations of these air-sea parameters with wind speed (U) measured at 19.5 m above the sea surface are presented in Figures 9A–C. Regression curves were chosen for each data comparison in Figures 9A–C on the basis of best overall fit and previously published relationships. The power-law regression employed for the whitecap results is suggested by theoretical considerations,[21] and the resulting exponent of 3.55 falls within the range of 3.10 to 3.75 reported by previous investigators.

In general, a fair amount of scatter is evident in the wave-breaking and whitecap observations. As discussed, it can be attributed in part to wind-history effects, surface wave-field variability, including swell interactions, and various other properties such as atmospheric stability,

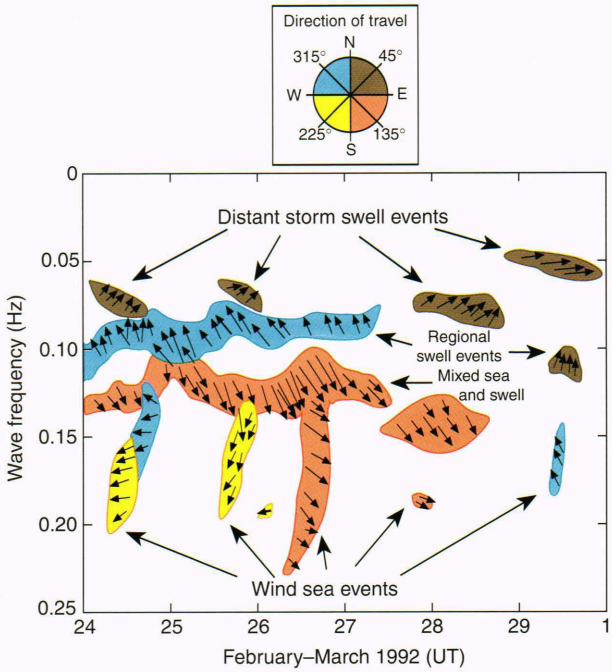

Figure 8. Surface-wave vector history showing the evolution of various wave systems during Critical Sea Test 7. The extreme complexity of the Gulf of Alaska wave climate is obvious; wind seas often coexisted with multiple swell systems arriving from scattered directions.

sea-surface temperature, and upper-ocean structure. It is noteworthy that the wave-breaking frequency and whitecap fraction comparisons (Figs. 9A and 9B) each reveal that wave-breaking activity increases abruptly when the winds surpass 5 m/s.

The comparison of bubble depth and wind speed in Figure 9C indicates that bubbles penetrated the mixed layer to depths of nearly 20 m. Occurring during the high winds associated with the 25 to 26 February storm, this exceptionally deep invasion of bubbles was probably due to large-scale Langmuir circulation cells driven by the surface storm conditions and additionally supported by the exceptionally deep (>100 m) mixed layer existing at that time (D. Farmer, pers. comm., 1992).

Note in Figures 9A–C that both wave-breaking indicators (breaking frequency and whitecap fraction) correlate poorly with wind speed, whereas bubble-cloud depth correlates moderately well with the wind. The next section further explores this result and includes an investigation of wind-history effects on these quantities.

ANALYSIS

A slow response of the sea surface to wind action is expected since water has an inertia much greater than that of air. As a result, air-sea conditions represent an integrated effect of the wind forcing. To determine the importance of wind history during CST-7, selected wind-forcing parameters were averaged back in time and correlated with the wave-height, wave-breaking, and bubble-cloud indicators. Initially, wind speed (U), U^2, U^3, friction velocity (u^*), and wind stress (τ) were linearly back-averaged over selected time periods ranging from 0.25 to

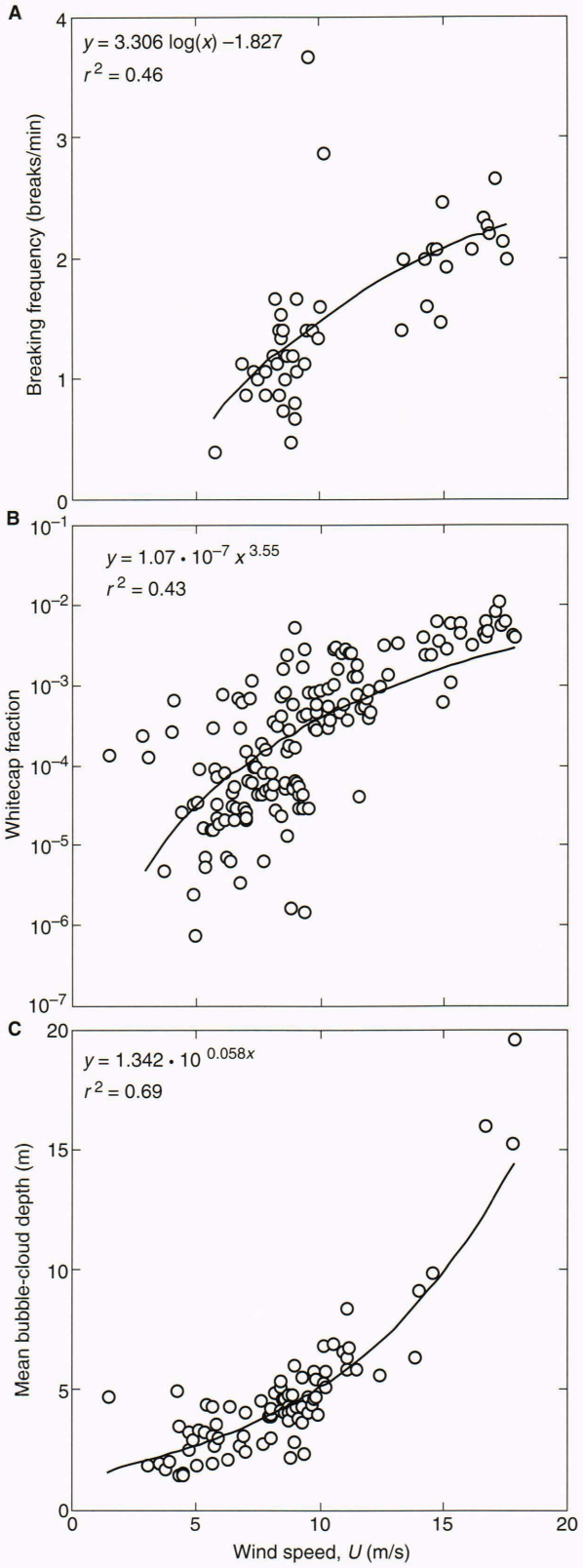

Figure 9. Correlation of air-sea parameters with wind speed (at 19.5 m above the sea surface). **A.** Wave-breaking frequency. **B.** Whitecap fraction. **C.** Mean bubble-cloud depth. Wave breaking and whitecaps are poorly correlated with wind, whereas bubble-cloud development is moderately well described by the wind field. Equations are given for the best fits to the data, along with the correlation coefficients (r^2).

20 h. The back-averages were then correlated with significant wave height, wave-breaking frequency, whitecap fraction, and bubble-cloud depth. Second-order polynomial regressions were calculated for all data comparisons except the whitecap fraction correlations, for which a power-law fit was chosen for reasons already stated.

In almost all situations, the atmospheric forcing parameter U^3 provided the best fit to each air-sea descriptor. That result is reasonable since energy flux considerations suggest a near cubic dependence of wind on the production of whitecaps.[22] The results of the U^3 correlations at back-average periods between 0 and 6 h appear in Figure 10. Regression coefficients (r^2) are plotted as a function of the back-average period so that optimal wind-history averaging time for each air-sea descriptor can be identified.

The relatively poor correlation of significant wave height (H_s) to the wind averages is attributed to the continual contribution of swells, mostly unaffected by the local wind, to the total wave height. As expected, both of the wave-breaking indicators (breaking frequency and whitecap fraction) behave similarly in that a poor correlation with instantaneous wind is remarkably improved with two to three hours of wind averaging. A surprise, however, is that the bubble-cloud depth correlations have an opposite trend. Excellent regressions of bubble-cloud depth with short-term average winds (0.5–1.5 h) degrade substantially with longer time averages. These comparisons suggest that the mixing processes that promote the distribution of subsurface bubbles, such as Langmuir circulation, respond more quickly to wind-speed changes than do the surface waves.

The wind-history studies indicate that in the Gulf of Alaska wintertime environment, the formation of deep bubble clouds is somewhat decoupled from the bubble supply mechanism of wave breaking. As further evidence, direct comparisons of breaking frequency and whitecap fraction to bubble-cloud depth appear in Figures 11A and 11B. Although the difficulties of obtaining overlapping measurements at sea (see Fig. 5) result in a limited data set for comparison, the results of Figures 11A and 11B suggest that wave breaking and bubble-cloud depths are poorly correlated, especially at elevated wind speeds when bubbles are driven deep by Langmuir circulation. It is likely that wave-breaking activity under winter conditions provides a near-continuous supply of bubbles to the upper ocean, whereas the deep penetration of the bubbles into the mixed layer is controlled by the development of large-scale circulation structures, such as Langmuir cells, initiated by the surface drift currents driven by high wind events.

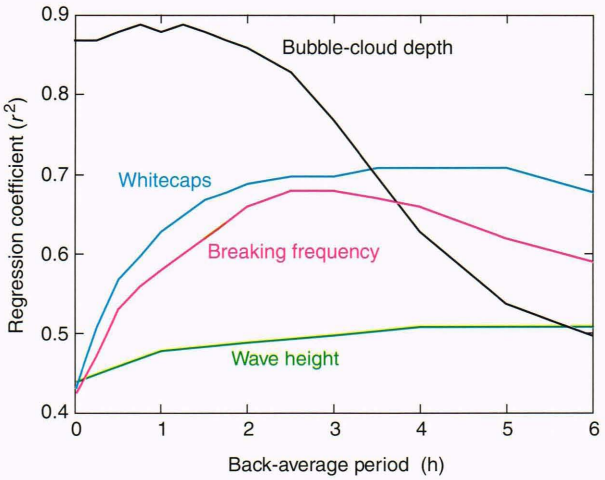

Figure 10. Results of air-sea parameter correlations with wind history (U^3). Wave breaking requires two- to three-hour wind back-averaging to attain a reasonable correlation with the wind, whereas bubble-cloud depth is more closely coupled with short-term (0.5–1.5 h) wind averages. Significant wave heights are poorly correlated at all wind-history averages because of the contaminating effect of swell.

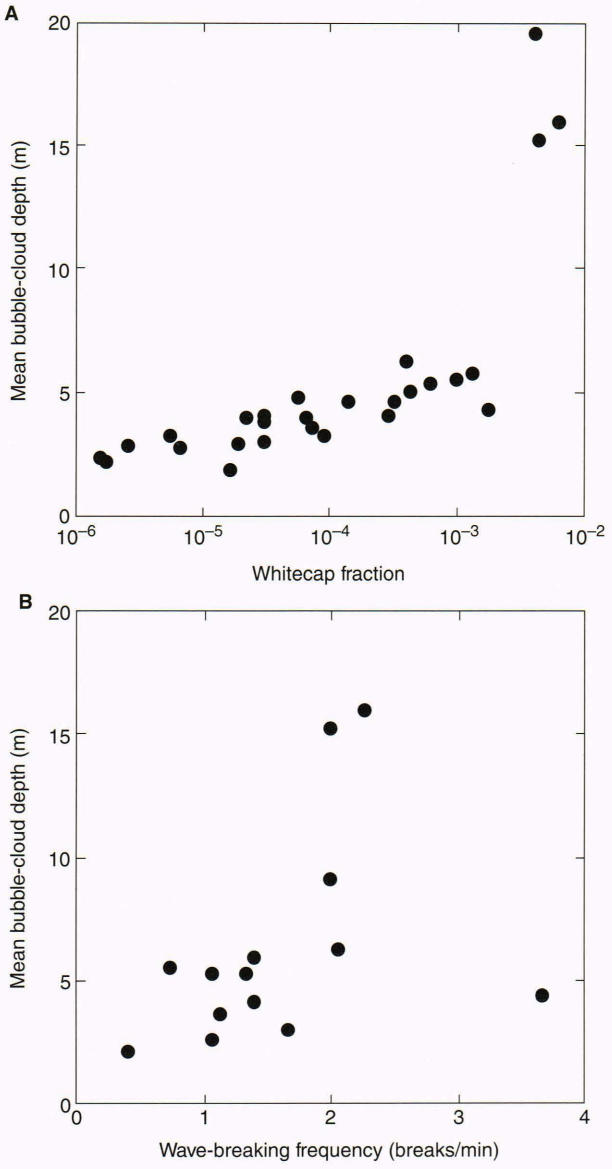

Figure 11. Direct correlation of bubble-cloud depth to the wave-breaking parameters. **A.** Whitecap fraction. **B.** Wave-breaking frequency. Although a limited data set, the results indicate that the formation of deep bubble clouds is somewhat decoupled from the bubble supply mechanism of wave breaking, especially when bubbles are driven deep by Langmuir circulations during elevated winds.

The CST-7 Phase 2 surface scatter and air-sea interaction experiment was probably the most successful experiment of this type ever performed. Concurrent measurements of low-frequency acoustic backscatter (50–1000 Hz), distant surface reverberation, biological (fish) scatter, subsurface bubble clouds, surface-wave features, mixed-layer attributes, and surface meteorology are allowing in-depth investigations into the nature of ocean surface scatter. It is anticipated that the results from this experiment will lead to the selection and use of more appropriate environmental descriptors in reverberation modeling, yielding significant improvements in overall acoustic prediction capability.

Incidentally, the production and evolution of subsurface bubbles have also been shown to be important components of the air-sea gas exchange process.[23,24] The accelerated transfer of gas by subsurface bubble penetration is not yet accounted for in the most widely accepted (thin-layer) air-sea flux models. It is anticipated that a new sea-state model that includes a refined understanding of the air-sea boundary mechanisms responsible for the production and evolution of subsurface bubbles would lead to improved air-sea gas flux predictions for use in regional and global climate investigations.

REFERENCES

[1] Tyler, G. D., "The Emergence of Low-Frequency Active Acoustics as a Critical Antisubmarine Warfare Technology," *Johns Hopkins APL Tech. Dig.* **13**(1), 145-159 (1992).

[2] Root, S. L., and Hanson, J. L. (eds.), *Critical Sea Test 7, Phase II Quick-Look Report*, The Johns Hopkins University Applied Physics Laboratory, Laurel, Md. (1992).

[3] Hanson, J. L., and Erskine, F. T. , "An Experiment to Study the Influence of the Air-Sea Boundary Zone on Underwater Acoustic Reverberation," in *MTS '92*, Marine Technology Society, Washington, D.C. (1992).

[4] Henyey, F. S., "Acoustic Scattering from Ocean Microbubble Plumes in the 100 Hz to 2 kHz Region," *J. Acoust. Soc. Am.* **90**(1), 399-405 (1991).

[5] Roy, R. A., Carey, W., Nicholas, M., Schindall, J., and Crum, L., "Low-Frequency Scattering from Submerged Bubble Clouds," *J. Acoust. Soc. Am.* **92**(5), 2993-2996 (1992).

[6] Ogden, P. M., and Erskine, F. T., An Empirical Prediction Algorithm for Low-Frequency Acoustic Surface Scattering Strengths, Naval Research Laboratory, Washington, D.C. (1992).

[7] Stull, R. B., *An Introduction to Boundary Layer Meteorology*, Kluwer Academic Publishers, Dordrecht, p. 666 (1988).

[8] Miles, J. W., "On the Generation of Surface Waves by Shear Flows. Part 2," *J. Fluid Mech.* **6**, 568-582 (1959).

[9] Huang, N. E., "On Surface Drift Current in the Ocean," *J. Fluid Mech.* **91**, 191-208 (1979).

[10] Lamarre, E., and Melville, W. K. "Air Entrainment and Dissipation in Breaking Waves," *Nature* **351**, 469-472 (1991).

[11] Mitsuyasu, H., "Wave Breaking in the Presence of Wind Drift and Opposed Swell," in *Breaking Waves*, M. L. Banner and R. H. J. Grimshaw (eds.), Springer-Verlag, Berlin, pp. 147-153 (1992).

[12] Thorpe, S. A., "On the Clouds of Bubbles Formed by Breaking Wind-Waves in Deep Water, and Their Role in Air-Sea Gas Transfer," *Philos. Trans. R. Soc. London* **A 304**, 155-210 (1982).

[13] Smith, J., Pinkel, R., and Weller, R., "Velocity Structure in the Mixed Layer during MILDEX," *J. Phys. Oceanogr.* **17**, 425-439 (1987).

[14] Smith, J. A., "Observed Growth of Langmuir Circulation," *J. Geophys. Res.* **97**(C4), 5651-5664 (1992).

[15] Leibovich, S., "The Form and Dynamics of Langmuir Circulations," *Annu. Rev. Fluid Mech.* **15**, 391-427 (1983).

[16] White, L. H., and Hanson, J. L., "Development of a Shipboard Air-Sea Dynamics System," in *Oceans '91*, IEEE, New York (1991).

[17] Marsden, R. F., and Juszko, B.-A. "An Eigenvector Method for the Calculation of Directional Spectra from Heave, Pitch and Roll Buoy Data," *J. Phys. Oceanogr.* **17**(12), 2157-2167 (1987).

[18] Gerling, T. W., "Partitioning Sequences and Arrays of Directional Ocean Wave Spectra into Component Wave Systems." *J. Atmos. Oceanic Technol.* **9**, 444-458 (1992).

[19] Monahan, E. C., "Occurrence and Evolution of Acoustically Relevant Subsurface Bubble Plumes and Their Associated, Remotely Monitorable, Surface Whitecaps," in *Natural Physical Sources of Underwater Sound: Sea Surface Sound (2)*, B. R. Kerman (ed.), Kluwer Academic Publishers, Boston, pp. 503-517 (1993).

[20] Vagle, S., and Farmer, D. M., "The Measurement of Bubble-Size Distributions by Acoustical Backscatter." *J. Atmos. Oceanic Technol.* **9**, 630-644 (1992).

[21] Phillips, O. M., "Spectral and Statistical Properties of the Equilibrium Range in Wind-Generated Gravity Waves," *J. Fluid Mech.* **156**, 505-531 (1985).

[22] Wu, J., "Individual Characteristics of Whitecaps and Volumetric Description of Bubbles." *IEEE J. Oceanic Eng.* **17**(1), 150-158 (1992).

[23] Wallace, D. W. R., and Wirick, C. D., "Large Air-Sea Gas Fluxes Associated with Breaking Waves," *Nature* **356,** 694-696 (1992).

[24] Farmer, D. M., McNeil, C. L., and Johnson, B. D., "Evidence for the Importance of Bubbles in Increasing Air-Sea Gas Flux," *Nature* **361**, 620-623 (1992).

ACKNOWLEDGMENTS: This work has been graciously supported by the Office of Naval Research (ONR Code 04) and the Space and Naval Warfare Systems Command (SPAWAR Code 182-32). Valuable data sets were obtained from Richard F. Marsden (wave spectra, wind stress), Edward C. Monahan (whitecap fractions), Johannes R. Gemmrich (wave-breaking statistics), and Svein Vagle (bubble depths). Susanne Hasselmann provided an early version of the wave partitioning code. Finally, Larry H. White, Charles C. Cooke, and Michele E. D'Anna aided in the processing and analysis of the wind records.

THE AUTHOR

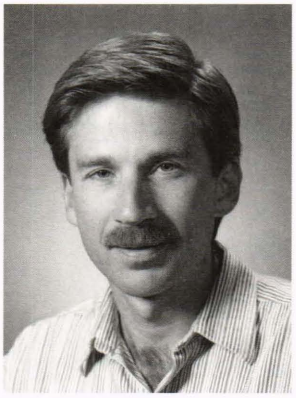

JEFFREY L. HANSON received the B.S degree from Florida Institute of Technology in 1981 and the M.S. degree from the University of South Florida in 1985. He is currently working part-time on a Ph.D. degree at The Johns Hopkins University. Mr. Hanson has been a physical oceanographer at APL since 1985 and has led environmental measurement and analysis projects since 1986. He directed the development of both the System for At-Sea Environmental Analysis and the Air-Sea Dynamics System. His current research interests focus on the air-sea boundary zone and, in particular, mechanisms related to breaking waves, subsurface bubbles, and acoustic scatter. He was selected as the Merle A. Tuve Fellow to continue his air–sea research at The Johns Hopkins University for the academic year 1993-94. Mr. Hanson is a member of the Acoustical Society of America, the American Geophysical Union, IEEE (Ocean Engineering), and The Oceanography Society.